Journal of Cellular and Molecular Medicine
A JOURNAL OF TRANSLATIONAL MEDICINE

J. Cell. Mol. Med. Vol 15, No 10, 2011 pp. 2082-2094

Systemic transplantation of human adipose-derived stem cells stimulates bone repair by promoting osteoblast and osteoclast function

Kyunghee Lee [a, b, #], Hyunsoo Kim [a, b, #], Jin-Man Kim [a, b], Jae-Ryong Kim [b, c], Keuk-Jun Kim [d], Yong-Jin Kim [e], Se-Il Park [f], Jae-Ho Jeong [g], Young-mi Moon [g], Hyun-Sook Lim [h], Dong-Won Bae [i], Joseph Kwon [j], Chang-Yong Ko [k], Han-Sung Kim [k], Hong-In Shin [l], Daewon Jeong [a, b, *]

[a] *Department of Microbiology, Yeungnam University College of Medicine, Daegu, Korea*
[b] *Aging-associated Vascular Disease Research Center, Yeungnam University College of Medicine, Daegu, Korea*
[c] *Department of Biochemistry and Molecular Biology, Yeungnam University College of Medicine, Daegu, Korea*
[d] *Department of Clinical Pathology, Taekyeung College, Gyeungsan, Korea*
[e] *Department of Pathology, Yeungnam University College of Medicine, Daegu, Korea*
[f] *Department of Orthopedic Surgery, Yeungnam University College of Medicine, Daegu, Korea*
[g] *Noblesse Plastic Surgery & Stem Tec Korea, Daegu, Korea*
[h] *Department of Public Health Administration, Hanyang Women's University, Seoul, Korea*
[i] *Central Instrument Facility, Gyeongsang National University, Jinju, Korea*
[j] *Gwangju Center, Korea Basic Science Institute, Gwangju, Korea*
[k] *Department of Biomedical Engineering, College of Health Science, Institute of Medical Engineering, Yonsei University, Wonju, Korea*
[l] *IHBR, Department of Oral Pathology, School of Dentistry, Kyungpook National University, Daegu, Korea*

Received: August 20, 2010; Accepted: November 2, 2010

Abstract

Systemic transplantation of adipose-derived stem cells (ASCs) is emerging as a novel therapeutic option for functional recovery of diverse damaged tissues. This study investigated the effects of systemic transplantation of human ASCs (hASCs) on bone repair. We found that hASCs secrete various bone cell-activating factors, including hepatocyte growth factor and extracellular matrix proteins. Systemic transplantation of hASCs into ovariectomized mice induced an increased number of both osteoblasts and osteoclasts in bone tissue and thereby prevented bone loss. We also observed that conditioned medium from hASCs is capable of stimulating proliferation and differentiation of osteoblasts *via* Smad/extracellular signal-regulated kinase (ERK)/JNK (c-jun NH_2-terminal kinase) activation as well as survival and differentiation of osteoclasts *via* ERK/JNK/p38 activation *in vitro*. Overall, our findings suggest that paracrine factors secreted from hASCs improve bone repair and that hASCs can be a valuable tool for use in osteoporosis therapy.

Keywords: adipose-derived stem cell • osteoblast • osteoclast • osteoporosis • systemic transplantation

Introduction

Osteoporosis is a prevalent bone disease that is characterized by loss of bone mass and strength, leading to fragility fracture [1]. Osteoblasts, which are derived from mesenchymal stem cells (MSCs), are ultimately responsible for bone formation; osteoclasts are derived from pluripotent haematopoietic cells and are capable of resorbing bone. During adult life, bone is continuously remodelled by orchestrated cross-talk between osteoblasts and osteoclasts [2], and an imbalance in their function results in decreased bone quality, most commonly represented by the osteoporotic phenotype. A relatively higher bone resorption activity by osteoclasts than bone formation activity by osteoblasts leads to bone loss. High- and low-turnover osteoporotic

[#]These authors contributed equally to this work.
*Correspondence to: Daewon JEONG,
Department of Microbiology, Yeungnam University College of Medicine, Daegu 705-717, Korea.
Tel.: +82-53-620-4365
Fax: +82-53-653-6628
E-mail: dwjeong@ynu.ac.kr

doi: 10.1111/j.1582-4934.2010.01230.x

phenomena are known to be achieved by excessive bone resorption and reduced bone formation during bone remodelling, respectively [2].

Recent progress in stem cell biology has provided a promising strategy for treatment of multiple degenerative disorders [3]. In particular, adult stem cells have emerged as an important issue due to the potential for use of their *ex vivo* expanded progenies in cell-based regenerative medicine, tissue engineering and cancer therapy [4]. Adult stem cells participate in replenishment of cells that are lost during regeneration of damaged tissue, as well as in normal tissue development. MSCs, which possess unique immunosuppressive and anti-inflammatory properties and a capacity for homing to injured tissues, have been isolated from various tissues, including bone marrow, adipose, hair follicles, spleen, placenta, umbilical cord blood, foetal liver and lung [4]. MSCs obtained from adipose tissues could constitute a promising source of cells for use in cell-based therapy and tissue engineering [5]. Therapeutic potential for bone regeneration by systemic transplantation of genetically manipulated MSCs co-expressing C-X-C chemokine receptor type 4 (CXCR4) and Cbfa-1 in glucocorticoid-induced osteoporotic mice has been recently suggested [6].

The main benefits of adipose-derived stem cells (ASCs) in therapeutic applications, as compared with bone marrow-derived MSCs, are that adipose tissue is readily accessible and relatively abundant, and the stem cell population can be easily harvested by simple methods, such as lipoaspiration or surgical resection, and can be rapidly expanded *ex vivo* [7]. ASCs have also been shown to support differentiation of haematopoietic progenitors into myeloid and B lymphoid cells [8]. ASC-derived cellular therapy has been investigated with respect to a wide variety of human diseases, such as skeletal muscle disorders, cardiovascular disorders and diabetes mellitus, and in bioengineering for tissue regeneration [4]. Additive support of ASCs in tissue repair and regeneration has been reported to include differentiation into a proper cell lineage and paracrine mechanisms mediated by secreted cytokines and growth factors [5]. Growing evidence indicates that paracrine factors play a critical role in ASC-induced tissue repair [9, 10]. Bioactive levels of multiple paracrine factors, including hepatocyte growth factor (HGF), vascular endothelial growth factor, nerve growth factor, insulin-like growth factor-1 (IGF-1), transforming growth factor-β, basic fibroblast growth factor and granulocyte macrophage colony-stimulating factors are known to be released by ASCs [11]. Moreover, conditioned media obtained from ASCs have been found to protect against cerebellar granule neuron apoptosis [12].

Considering the fact that the pathogenetic mechanisms underlying osteoporosis cover multiple sets of dynamic parameters, a systemic approach using stem cell transplantation is attractive for treatment of osteoporosis. In the present study, we investigated the question of whether systemically transplanted human ASCs (hASCs) could restore bone function and structure in an ovariectomized (OVX)-induced osteoporotic mouse model.

Materials and methods

Isolation and culture of hASCs

Human subcutaneous adipose tissues were obtained under approval from the institutional review board of Yeungnam University Medical Center. The lipoaspirate was incubated with collagenase type I solution (Worthington Biochemical, Lakewood, NJ, USA) for 1 hr at 37°C, and filtered through 500 and 250 μm filters. Following centrifugation, the stromal vascular fraction was resuspended in DMEM (HyClone, Logan, UT, USA) supplemented with 10% foetal bovine serum (FBS) (HyClone), 100 U/ml penicillin and 100 μg/ml streptomycin. Cells were cultured under a humidified atmosphere of 5% CO_2 at 37°C and used for experiments at passages 3 to 5.

Preparation of conditioned media

hASCs and human embryonic kidney (HEK)293T fibroblast cells were seeded on a 100 mm dish in DMEM supplemented with 10% foetal bovine serum. At 90% confluence, cells were washed three times with phosphate-buffered saline and the medium was replaced with serum-free medium. After 1 hr, the medium was removed and fresh serum-free medium was added. As a control, conditioned media from hASCs (hASC-CM) and HEK293T cells (HEK293T-CM) were collected at 60 and 24 hrs after culture, respectively, which did not cause cell death for the indicated times (data not shown). Media were centrifuged at 300 × *g* for 5 min., and filtered through a 0.22 μm syringe filter. For *in vitro* cultures of osteoblasts and osteoclasts in hASC-CM, equal volumes of hASC-CM and α-MEM (HyClone) with FBS adjusted to 10% were used without concentration (50% hASC-CM). HEK293T-CM/α-MEM (1:1) or DMEM/α-MEM (1:1) was used as a control medium. For Western blot analysis and mass spectrometric identification of secreted proteins in hASCs, hASC-CM were concentrated 50-fold using an Amicon Ultra-15 (Millipore, Bedford, MA, USA) with a 10,000 molecular weight cutoff.

RT-PCR, Western blotting and ELISA assay

For detection of mRNA level, total RNA was isolated with TRIzol (Invitrogen, Carlsbad, CA, USA), according to the manufacturer's instructions. About 2 μg of total RNA was reverse transcribed using Moloney murine leukaemia virus reverse transcriptase (Promega, Madison, WI, USA) with oligo dT at 42°C for 1 hr. Detailed information on PCR, including primer sequences and cycles, is provided in Table S1. For Western blotting, cells were lysed by addition of lysis buffer containing 20 mM Tris-HCl, pH 7.5, 150 mM NaCl, 1% NP-40, 0.5% Na-deoxycholate, 1 mM ethylenediaminetetraacetic acid (EDTA), 0.1% SDS, protease inhibitors (Complete tablets, Roche Molecular Biochemicals, Mannheim, Germany), 1 mM Na_3VO_4 and 1 mM NaF. Proteins were separated by 10% SDS-PAGE, transferred to a nitrocellulose membrane and probed with specific antibodies. All antibodies used in this study are described in the Supporting Information. Protein levels of HGF in serum were measured using the Quantikine ELISA Kit (R&D Systems, Inc., Minneapolis, MN, USA). Urine deoxypyridinoline (DPD) was assayed by competitive enzyme immunoassay using the MicroVue DPD EIA kit (Quidel Corporation, Santa Clara, CA, USA).

Protein identification using mass spectrometry

As previously described, proteins obtained from SDS-PAGE gels or from concentrated hASC-CM were identified using mass spectrometry (Gwangju Center, Korea Basic Science Institute, Korea) [13]. Detailed methods are described in the Supporting Information.

Microcomputed tomography and histological analysis of bone

A total of 2×10^6 cells were injected into sham-operated or OVX female ddY mice (8 weeks old, Central lab animal, Korea) *via* tail vein on post-operative day 4 and killed at day 24 after injection ($n = 6$ per group). Microcomputed tomography (μCT) and histological analysis were performed, as reported previously [14, 15]. Trabecular morphometry within the proximal tibia was quantified using high resolution μCT (Skyscan 1076 μCT, Aartselaar, Belgium). From μCT data, bone loss indices, including bone volume/total volume (BV/TV), trabecular number (Tb.N) and bone mineral density (BMD) were assessed. For analysis of bone formation, mice were injected with calcein (10 mg/kg) on post-operative day 14 and day 21 and were killed at post-operative day 24. For histological evaluation, serial 5-μm-thick sagittal sections were made using a microtome. Haematoxylin and eosin staining was used for detection of osteoblasts and tartrate resistant acid phosphatase (TRAP) staining was used for visualization of osteoclasts. Histological images were analysed by an Aperio ScanScope Model T3 and ImageScope software (Aperio Technologies, Inc., Vista, CA, USA). All animal procedures were approved by the institutional review board of Yeungnam University Medical Center and were in accordance with the Guide for the Care and Use of Laboratory Animals.

Detection of hASCs after intravenous injection

After 8-week-old female ddY mice had been OVX, hASCs (2×10^6 cells/mouse) labelled with iron oxide (Ferridex, Berlex Laboratories, Inc., Wayne, NJ, USA) were injected into OVX mice *via* tail vein on post-operative day 4 and killed at day 24 after injection. Bone tissues were fixed and decalcified with EDTA solution. After washing, paraffin-embedded specimens were sectioned, deparaffinized, incubated with 1% potassium ferrocyanide in 1% HCl for 30 min. and counterstained with nuclear fast red. Six animals were included in each group.

In vitro assays of osteoblast differentiation, adhesion and spreading

Primary osteoblast cells were prepared from the calvaria of 3-day-old C57BL/6J mice (Central lab animal) and cultured with α-MEM containing antibiotics and 10% FBS at 37°C in 5% CO_2. Osteoblastic differentiation in the absence or presence of hASC-CM and/or 1,25-dihydroxyvitamin D_3 ($VitD_3$) was monitored for 24 days. For mineralization assay, we used 1×10^4 cells per well in 48-well plates. For quantification of calcium, mineralized osteoblasts were decalcified with 0.6 M HCl and calcium ion concentration was determined using a QuantiChrom™ calcium assay kit (DICA-500, BioAssay Systems, Hayward, CA, USA), according to the manufacturer's procedures. In order to normalize this assay, the remaining cells were lysed in 0.1 M NaOH/0.1% SDS, and protein concentration was determined using Bio-Rad protein assay reagent (Bio-Rad, Hercules, CA, USA). Detailed methods for cell adhesion and spreading assays are described in Supporting Information.

In vitro assays of osteoclast differentiation and function

Bone marrow-derived monocytes were isolated from the tibia and femur of 6-week-old C57BL/6J mice (Central lab animal) by flushing the bone marrow cavity. Osteoclast precursors were prepared as described [16] and detailed methods are described in the Supporting Information. To induce osteoclast differentiation, osteoclast precursors were cultured with 5 ng/ml of macrophage colony-stimulating factor (M-CSF) for 12 hrs, and the medium was then replaced with either control medium (50% HEK293T-CM in α-MEM or 50% DMEM in α-MEM) or 50% hASC-CM (50% hASC-CM in α-MEM) in the absence or presence of M-CSF (30 ng/ml) or receptor activator for nuclear factor κB ligand (RANKL, 50 ng/ml) for the indicated time periods. When cultured in 50% hASC-CM in α-MEM, the final concentration of FBS was adjusted to 10%. For positive controls, osteoclast precursor cells were cultured with M-CSF (30 ng/ml) and RANKL (100 ng/ml) for 3 to 4 days. For identification of osteoclasts, TRAP staining was performed with an Acid Phosphatase Kit (Sigma-Aldrich, St. Louis, MO, USA), according to the manufacturer's instructions. A TRAP solution assay was performed by addition of 5.5 mM *P*-nitrophenyl phosphate, a colorimetric substrate, in the presence of 10 mM sodium tartrate at pH 5.2. The reaction product was quantified by measurement of optical absorbance at 405 nm.

Statistical analysis

Data are presented as means $\pm$ S.D. from at least three independent experiments. Differences were considered statistically significant if *P*-value was less than 0.05. Statistical analyses were performed with the two-tailed Student's t-test for analysis of differences among groups.

Results

Characterization of hASCs

Cell surface marker expression by hASCs isolated from human adipose tissue was characterized. Flow cytometric analysis of hASCs revealed that high levels of MSC-related antigens CD13, CD29, CD44, CD90 and CD166 were expressed; however, haematopoiesis-related antigens CD31, CD34, CD117 and human leucocyte antigen CD45 were not expressed (Fig. S1). In additional, the ability of hASCs to differentiate into osteoblast, chondrocyte and adipocyte lineages at passage 3 was experimentally confirmed by von Kossa staining, Alcian blue staining and Oil red O staining, respectively (Fig. S2). These results showed that hASCs have multilineage potential and characteristics of MSCs.

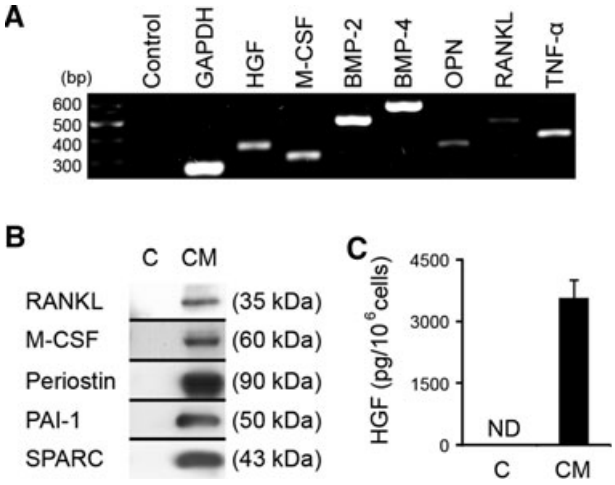

Fig. 1 Gene expression analysis of bone-related factors in hASCs and protein identification in hASC-CM. (**A**) mRNA levels for bone-related genes in hASCs. The mRNA expression profile of genes representative of osteoblast and osteoclast function was analysed using RT-PCR. The level of glyceraldehyde 3-phosphate dehydrogenase (GAPDH) served as an internal control for equal loading, and a PCR reaction without specific primers was used as a negative control. The gel is representative of three independent experiments. HGF: hepatocyte growth factor; M-CSF: macrophage colony-stimulating factor; BMP-2: bone morphogenetic protein 2; BMP-4: bone morphogenetic protein 4; OPN: osteopontin; RANKL: receptor activator for nuclear factor κB ligand; TNF-α: tumour necrosis factor-α. (**B**) Protein expression levels of bone-related genes. Levels of RANKL, M-CSF, periostin, plasminogen activator inhibitor 1 (PAI-1) and SPARC in hASC-CM concentrated 50-fold were determined by Western blot analysis. C: control medium; CM: hASC-CM. (**C**) Secretion of HGF from hASCs was measured by ELISA. Data are normalized as pg per 10^6 cells and are expressed as means ± S.D. ($n = 3$). ND: not detected.

Gene and protein expression of bone-related factors in hASCs and mass spectrometric identification of proteins secreted from hASCs

It is well established that hASCs have the ability to secrete a variety of cytokines, including angiogenic, anti-apoptotic and pro-inflammatory factors [11]. In this study, we examined expression and secretion of bone-related growth factors and cytokines in hASCs. Using RT-PCR, we observed expression of genes encoding HGF, M-CSF, bone morphogenetic protein 2 (BMP-2), BMP-4, osteopontin, RANKL and tumour necrosis factor-α in hASCs (Fig. 1A). Secretion of RANKL and M-CSF, which are essential for osteoclastogenesis, and HGF, which is known to increase DNA synthesis and proliferation of osteoblasts and osteoclasts [17], were confirmed in hASC-CM using Western blotting and ELISA (Fig. 1B and C).

To determine whether other proteins that affect bone function were present in hASC-CM, the secretome of primary hASC cultures was analysed using both gel-based and non-gel based approaches. First, SDS-PAGE combined with matrix-assisted laser desorption/ionization time-of-flight/time-of-flight mass spectrometry was used for protein identification in hASC-CM. Tryptic peptides from each band were identified using peptide mass fingerprinting and peptide sequencing, identifying 33 proteins in hASC-CM (Table S2). Second, we subjected the proteins of hASC-CM to in-solution tryptic digestion and nanoLC-tandem mass spectrometry, and identified 23 proteins in hASC-CM (Table S3). Table 1 shows a list of a total of 43 proteins identified by gel- and non-gel-based methods. Thirty-three proteins (77%) contained a predicted secretion signal peptide, and several proteins were reported to be involved in bone function. For example, secreted protein acidic and rich in cysteine (SPARC), periostin and fibronectin are known to stimulate proliferation and differentiation of osteoblasts [18–20]; β_2-microglobulin and thrombospondin-1 are involved in stimulation of osteoclast formation and function [21, 22]. The presence of some proteins identified in mass spectrometric analysis, such as periostin, plasminogen activator inhibitor 1 and SPARC was validated using Western blotting (Fig. 1B). Combined results from RT-PCR, Western blotting, ELISA and mass spectrometric protein identification demonstrated the release by hASCs of a variety of proteins and cytokines related to bone function, suggesting that paracrine factors produced by hASCs might possibly play an important role in bone remodelling and repair.

Effects of systemic transplantation of hASCs on OVX-induced bone loss

We performed μCT analysis to determine the impact of hASCs on OVX-induced osteoporotic mice (Fig. 2A). Systemic transplantation of hASCs into OVX mice prevented OVX-induced bone loss in mice. When compared with OVX mice, bone loss indices, including bone volume fraction, trabecular number and BMD in hASC-transplanted OVX mice were restored to normal. The recovery effect of hASCs on bone loss was confirmed by measurement of the concentration of urinary DPD, a useful marker of bone resorption. Compared with OVX mice, a significantly lower level of urinary DPD was exhibited by hASC-transplanted OVX mice (Fig. 2B). Mineral apposition rate and bone formation rate, as measured by calcein label-based analysis, were restored to the level of sham-operated mice in hASC-transplanted OVX mice (Fig. 2C). Of particular interest, histological analysis showed that the numbers of both osteoblasts and $TRAP^+$ osteoclasts adhering to trabecular bone surfaces were increased in hASC-transplanted OVX mice compared with sham and control OVX mice (Fig. 2D), suggesting that systemic transplantation of hASCs in OVX mice might affect proliferation or differentiation of osteoblasts and osteoclasts.

HGF that play important roles in bone formation and remodelling [17, 23] were expressed by hASCs (Fig. 1). Consistently, serum level of human HGF was markedly higher in hASC-transplanted OVX mice than in control OVX mice (Fig. 2E). Because oestrogen plays a critical role in OVX-induced bone loss [24], we explored the ovarian and uterine status of recipient mice (Fig. S3). Oestrogen-deficient OVX mice showed decreases in uterine weight and diameter. No significant differences in ovarian and uterine

Table 1 Mass spectrometric identification of proteins secreted by hASCs

Protein (accession number)	SignalP*	Bone-related function	Protein (accession number)	SignalP	Bone-related function
Fibronectin (Q9UMK2)	0.997	Osteoblast survival and differentiation [20]	Collagen α_1 (I) chain (Q9UML6)	0.999	Osteoblast maturation and differentiation [42]
Collagen α_2 (I) chain (P08123)	0.997	Osteoblast maturation and differentiation [42]	Thrombospondin-2 (P35442)	1.000	Osteoblast differentiation [43]
Collagen α_1 (III) chain (P02461)	0.999		Collagen α_1 (VI) chain (P12109)	1.000	
SR calcium ATPase 1 (O14983)			Thrombospondin-1 (P07996)	0.994	Osteoclast function [22]
α-actinin-1 (P12814)			Protein FAM40A (Q5VSL9)		
Periostin (Q15063)	0.999	Osteoblast proliferation and differentiation [19]	β ig-h3 (Q15582)	1.000	Osteoblast adhesion and differentiation [44]
Thrombospondin-5 (P49747)	1.000	Chondrocyte proliferation [45]	Matrix metalloproteinase 1 (P03956)	1.000	Osteoblast differentiation [46]
72 kD type IV collagenase (P08253)	1.000	Bone cell growth and proliferation [47]	Plasminogen activator inhibitor 1 (P05121)	0.999	Bone mineralization and bone growth [48]
Albumin (P02768)	1.000		Moesin (P26038)		
Galectin-3-binding protein (Q08380)	1.000		Protein disulfide-isomerase (P07237)	1.000	
Fibulin-3 (Q12805)	0.999		Vimentin (P08670)		
EF-1-alpha 1 (P68104)			Serpin A12 (Q8IW75)	0.997	
Cathepsin L1 (P07711)	0.999	Bone resorption [49]	Cathepsin D (P07339)	1.000	Osteoblast calcification [50]
Glia-derived nexin (P07093)	0.995		Pentraxin-related protein PTX3 (P26022)	1.000	
β-actin (P60709)			Decorin (P07585)	1.000	
Follistatin-related protein 1 (Q12841)	1.000		Sulfhydryl oxidase 1 (O00391)	1.000	
IGF-binding protein 7 (Q16270)	0.998		Cathepsin B (P07858)	1.000	
Peptidyl-prolyl cis-trans isomerase B (P23284)	0.863		SPARC (P09486)	1.000	Osteoblast formation, maturation and survival [18]
Lumican (P51884)	1.000	Bone formation [51]	Metalloproteinase inhibitor 2 (P16035)	1.000	Osteoblast differentiation [52]
Transgelin (Q01995)			Peroxiredoxin-1 (Q06830)		
Metalloproteinase inhibitor 1 (P01033)		Bone turnover [53]	Protein S100-A6 (P06703)		
β_2-microglobulin (P61769)	1.000	Osteoclast formation [21]			

*SignalP indicates the probability score calculated with SignalP software.

status were observed in hASC-transplanted OVX mice and control OVX mice. From these data, we confirmed the effectiveness of our OVX surgeries and the oestrogen status in the OVX mice.

For detection of hASCs in OVX mice after systemic transplantation, hASCs labelled with iron oxide were transplanted into OVX-induced osteoporotic mice *via* tail vein injection on post-operative day 4 and mice were killed on day 24 after transplantation. Distribution of hASCs was assessed by Prussian blue staining. Iron-labelled transplanted cells were detected in the periosteum of recipient OVX mice (Fig. 2F).

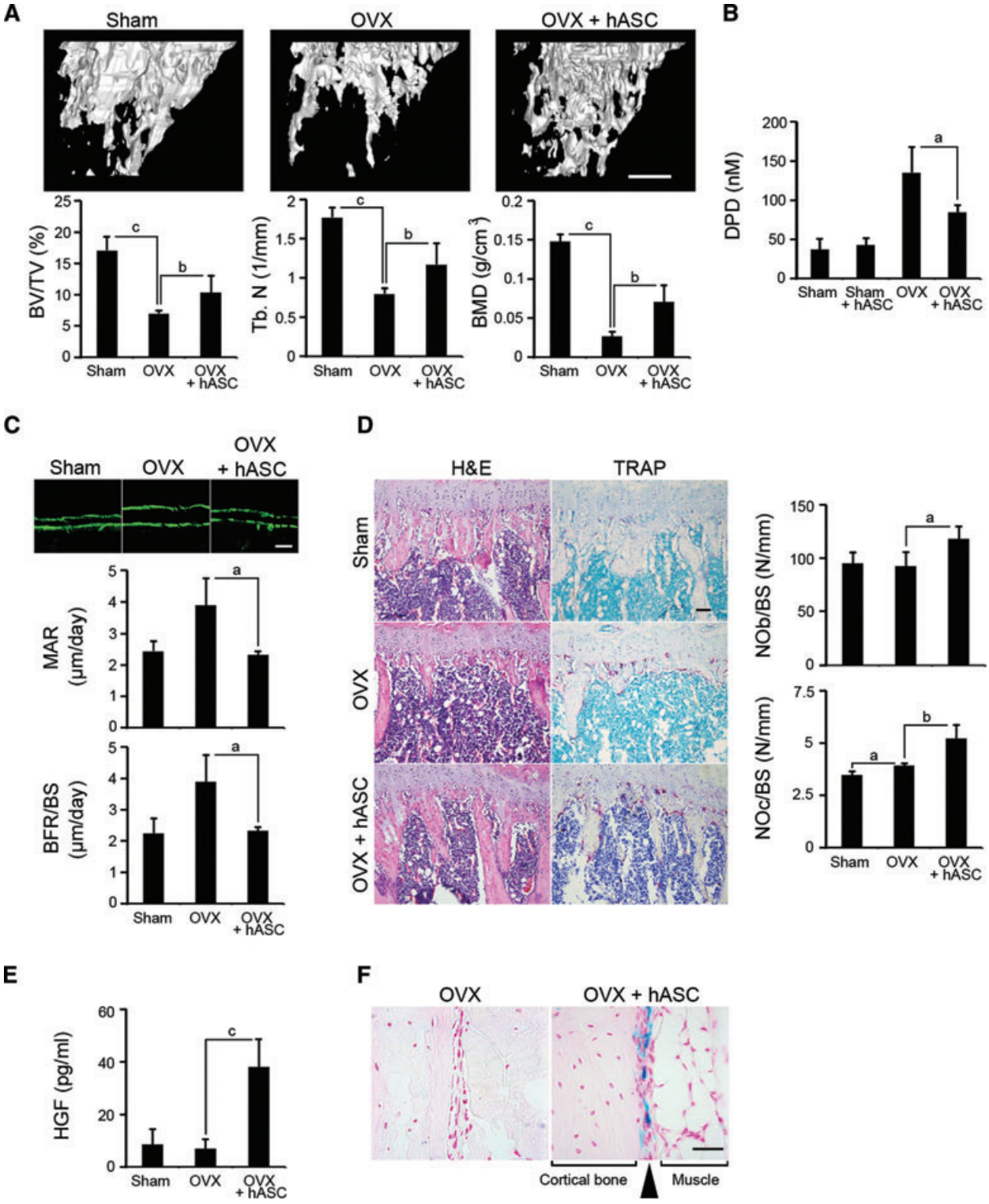

Fig. 2 *In vivo* effects of hASCs on OVX-induced osteoporotic mice. (**A**) μCT analysis of bone tissue. 3D reconstruction of tibiae from sham-operated (Sham) and OVX mice transplanted without or with hASCs (OVX and OVX + hASC) was analysed by μCT. Scale bar: 0.5 mm. Histograms represent 3D trabecular structural parameters in tibia: bone volume/total volume (BV/TV), trabecular number (Tb.N) and BMDs. Data represent mean ± S.D. ($n = 6$). (**B**) Urinary samples were obtained prior to killing and levels of DPD were measured by ELISA. Data represent mean ± S.D. ($n = 3$). (**C**) Mineral apposition rate and bone formation rate (BFR/BS) were measured by calcein labelling. Data represent mean ± S.D. ($n = 3$). Scale bar: 10 μm. (**D**) Histological analysis of tibiae from OVX mice systemically transplanted with or without hASCs. Osteoblasts and osteoclasts on the trabecular bone surface were visualized by haematoxylin and eosin and TRAP staining, respectively. The number of osteoblasts (NOb/BS) and osteoclasts (NOc/BS) is expressed as a cell number per mm of trabecular bone surface. Scale bar: 100 μm. Data represent mean ± S.D. ($n = 6$). The level of human HGF in serum of sham-operated or OVX mice with or without systemic transplantation of hASCs was determined by ELISA. (**E**) Data represent mean ± S.D. ($n = 3$). (**F**) Detection of hASCs in tibia of recipient OVX mice after systemic transplantation. hASCs (2×10^6 cells/200 μl) labelled with iron oxide were injected into OVX-induced osteoporotic mice *via* tail vein on post-operative day 4 and killed at day 24 after injection. Tissue sections from tibia of recipient mice were subjected to Prussian blue staining. Results shown are representative of three experiments. Scale bar: 50 μm. a: $P < 0.05$; b: $P < 0.01$; c: $P < 0.001$. 140 × 169 mm (300 × 300 DPI).

The effect of hASC-CM on osteoblast and osteoclast differentiation

Our results suggested that hASCs expressed and secreted bone-activating factors into the extracellular space, which are able to potentiate osteoblast and osteoclast differentiation (Fig. 1 and Table 1). In differentiation of osteoblasts and osteoclasts *in vitro*, it is established that $VitD_3$ and prostaglandin E2 can lead to osteoblast activation and mineralization and that RANKL, in combination with M-CSF, can induce multinucleated osteoclast formation from a macrophage lineage [14, 25, 26]. Thus, we assessed a stimulatory action of hASC-derived secreted factors in osteoblast and osteoclast differentiation under various combined cultures of bone cell-stimulating factors, hASCs-CM and HEK293T-CM as a control. Among various combinations, osteoblast cultures with hASC-CM and $VitD_3$ displayed mineral deposition, but did not with HEK293T-CM and $VitD_3$ (Fig. 3A). In additional, combined treatment of hASC-CM- and RANKL-induced differentiation of osteoclast precursors into $TRAP^+$ multinucleated cells (MNCs), whereas HEK293T-CM and RANKL treatment failed to induce their differentiation (Fig. 3B). These results indicate that osteoblastogenic factors present in hASC-CM can be substituted for prostaglandin E2, and that osteoclastogenic factors in hASC-CM can be substituted for M-CSF.

Stimulatory effect of hASC-CM on osteoblast proliferation and differentiation

Compared with sham-operated and OVX mice, systemic transplantation of hASCs into OVX mice resulted in an increase in the number of osteoblasts and osteoclasts on bone surfaces (Fig. 2D). To elucidate the molecular mechanisms responsible for *in vivo* results, we investigated the question of whether hASC-CM could affect the physiological properties of osteoblasts, including proliferation, adhesion, spreading and differentiation. We found that hASC-CM induced an increase in the osteoblast population, compared with the control medium (Fig. 4A). We also found that hASC-CM markedly promoted cell attachment and spreading, compared with the control medium (Fig. 4B and C). These enhanced activities of cell attachment and spreading were completely inhibited by EDTA, but not by heparin, suggesting that cell attachment and spreading in osteoblasts might be promoted by hASC-CM through a divalent cation-dependent mechanism. Whereas cultures supplemented with either hASC-CM or $VitD_3$ alone did not induce matrix mineralization of osteoblasts, addition of both hASC-CM and $VitD_3$ to cultures accelerated the mineralization of osteoblasts (Fig. 4D).

We next examined the effects of hASC-CM on signalling events in osteoblasts. As shown in Figure 4E, short-term treatment of osteoblasts with hASC-CM resulted in increased phosphorylation of receptor-regulated Smad 1/5/8, which is known to function as an intracellular mediator of osteoblast differentiation signalling [27], and to play an important role in early osteoblastogenesis [2]. However, neither phosphorylation nor expression levels of β-catenin in osteoblasts were altered by treatment with hASC-CM. In addition, we measured the activities of three MAPKs, ERK, c-jun NH_2-terminal kinase (JNK) and p38 in osteoblasts after long-term treatment with hASC-CM. Maximal activation of both ERK and JNK, which can, in part, stimulate osteoblast differentiation [28] was induced by day 3 after treatment with hASC-CM however, p38 was not affected (Fig. 4F).

Stimulatory effect of hASC-CM on osteoclast precursor survival and osteoclast differentiation

The combination of M-CSF and RANKL is indispensable for both survival and differentiation of osteoclast precursors [14]. To evaluate the effect of hASC-CM on survival and proliferation of osteoclast precursors, we counted the numbers of osteoclast precursors after exposure to hASC-CM. The number of osteoclast precursors cultured with hASC-CM was considerably higher than that of osteoclast precursors cultured with control medium (Fig. 5A). To determine whether hASC-CM could stimulate osteoclast differentiation, osteoclast precursors were cultured under the control medium or hASC-CM in the presence or absence of M-CSF or RANKL and stained with TRAP to detect mature osteoclasts. $TRAP^+$ MNCs were not detected in osteoclast precursors cultured

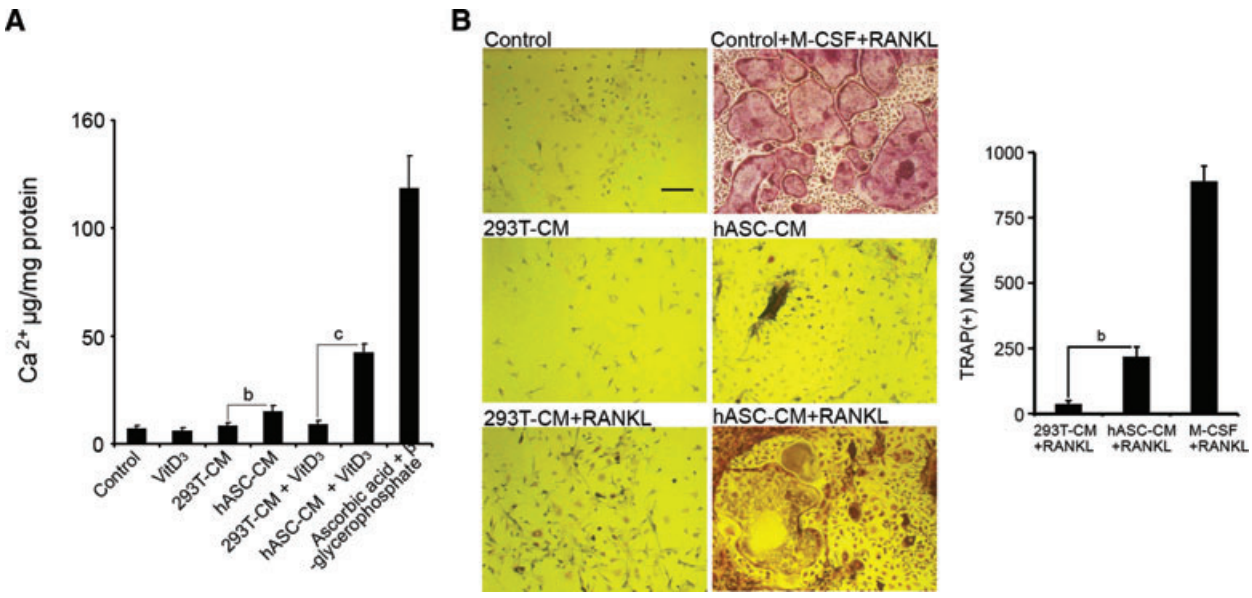

Fig. 3 Effects of hASC-CM on osteoblast and osteoclast differentiation. (**A**) Osteoblast mineralization. The mineralized extent of osteoblasts was quantified at day 24 after incubation of cells in 50% hASC-CM or 50% HEK293T-CM (as a control media) in the presence or absence of 10 nM $VitD_3$. For a positive control, osteoblasts were cultured in the presence of 100 μg/ml ascorbic acid and 10 mM β-glycerophosphate. Data represent mean ± S.D. ($n = 3$). (**B**) Osteoclast differentiation. Osteoclast precursors (5×10^4 cells per well in 48-well plates) were cultured for 8 days in 50% hASC-CM or 50% HEK293T-CM in the presence or absence of RANKL (50 ng/ml), as indicated. Cells were stained with TRAP and $TRAP^+$ MNCs (>3 nuclei) were counted under a light microscope. Representative images of three independent experiments are presented. Scale bar: 100 μm. b: $P < 0.01$; c: $P < 0.001$.

in hASC-CM in the presence or absence of M-CSF. However, osteoclast precursors cultured in hASC-CM in the presence of RANKL formed much higher numbers of $TRAP^+$ MNCs at day 9 of culture (Fig. 5B), consistent with the result shown in Figure 3B, suggesting that hASC-CM could efficiently support osteoclast formation in a manner similar to that of M-CSF. TRAP activity was also higher in osteoclast precursors cultured with hASC-CM than in osteoclast precursors cultured with control medium (Fig. 5C). mRNA expression of osteoclastic markers, such as cathepsin K, TRAP, NFATc1 and matrix metalloproteinase-9 were induced when osteoclast precursors were cultured in hASC-CM (Fig. 5D). All three major subfamilies of MAPKs, ERK, JNK and p38, which are known to play an important role in osteoclastogenesis, were activated immediately after hASC-CM treatment in osteoclast precursors (Fig. 5E). In contrast to the stimulatory action of hASC-CM in osteoblast adhesion and spreading (Fig. 4B and C), hASC-CM did not affect adhesion and spreading of osteoclast precursors (data not shown).

Discussion

Bioactive trophic factors secreted by ASCs have been reported to directly contribute to angiogenic and anti-apoptotic effects in ischemic limb disease, restoration of heart function and nerve sprouting following myocardial infarction, and skin wound healing [9, 10, 29, 30]. In this study, we showed that hASC-based therapy *via* systemic transplantation could be effective in bone repair by a mechanism predominantly mediated through secretion of paracrine factors by hASCs.

Osteoporosis is a chronic and complex disease involving an uncoupling between bone formation and bone resorption. Multiple pathogenetic mechanisms are involved in loss of bone mass and microarchitectural reduction of bone tissue in osteoporosis [1]. Bone repair is known to be a complex physiologic process that is regulated by several cell types, as well as the extracellular matrix and growth factors [31]. Secretion of important growth factors with potential for mediation of bone repair, including vascular endothelial growth factor, IGF-1 and TGF-β [32] from ASCs has been demonstrated [11]. In addition, we found that hASCs could express and secrete various cytokines, growth factors and proteins that are required for bone function and remodelling. These included M-CSF, RANKL, BMP-2, BMP-4, HGF and bone-related extracellular matrix proteins. Our *in vivo* results revealed that OVX-induced bone loss was restored by systemic transplantation of hASCs into recipient OVX mice. We further showed that hASC-injected OVX mice exhibited an increase in the number of both osteoblasts and osteoclasts. This could be explained by the balance between bone resorption and bone formation. The levels of bone resorption by osteoclasts did not exceed those of bone formation by osteoblasts, resulting in a net increase of bone mass. These findings indicate that hASCs can rescue oestrogen

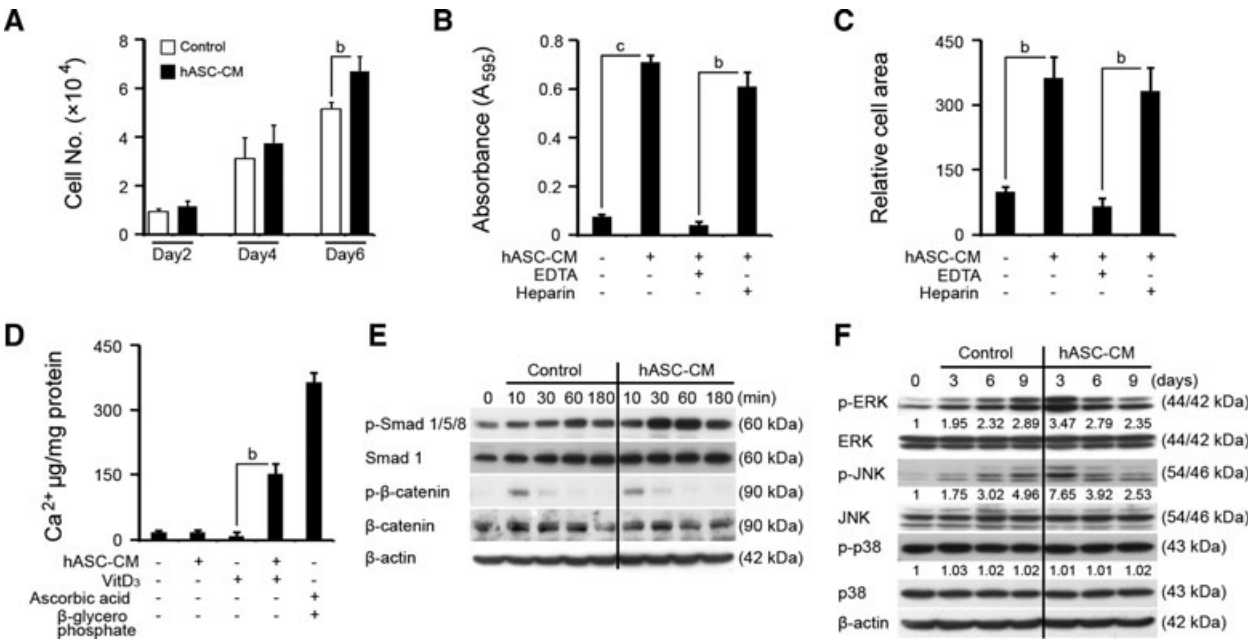

Fig. 4 Stimulatory action of hASC-CM in osteoblast proliferation, adhesion, spreading and differentiation. (**A**) Osteoblast proliferation. Following culture of osteoblasts (2×10^4 cells per well in 24-well plates) using a control medium (50% DMEM in α-MEM) or hASC-CM (50% hASC-CM in α-MEM) for the indicated times, trypan blue-excluded cells were counted using a haemocytometer under a light microscope. Data represent mean ± S.D. ($n = 3$). Cell adhesion (**B**) and spreading (**C**) assays were performed on osteoblasts incubated for 1 hr in the same media as in (**A**). For assessment of cell adhesion, cells were stained with crystal violet, dissolved in 2% SDS, and absorbance was measured at 595 nm. For assessment of cell spreading, cell area was measured using Image-Pro plus software. In inhibition experiments, cells were pre-incubated with either 5 mM EDTA or 100 μg/ml heparin at 37°C for 10 min. Values are expressed as the mean ± S.D. ($n = 3$). (**D**) Calcium content in osteoblasts. The extent of mineralization of osteoblasts (1×10^4 cells per well in 48-well plates) was quantified at day 24 after incubation of cells in the presence or absence of hASC-CM and/or 10 nM $VitD_3$. For a positive control, osteoblasts were cultured in the presence of 100 μg/ml ascorbic acid and 10 mM β-glycerophosphate. Data represent mean ± S.D. ($n = 3$). (**E**) and (**F**) Osteoblast-stimulating signals. Osteoblasts were stimulated with 50% hASC-CM for the indicated times and activation of Smad 1/5/8, β-catenin, ERK, JNK and p38, which are implicated in osteoblast differentiation and function, was assessed by Western blotting with specific antibodies. Numbers indicate the ratios of phosphorylated MAPKs to total MAPKs. β-actin was used as a loading control. Data are representative of three independent experiments. b: $P < 0.01$; c: $P < 0.001$.

deficiency induced bone loss by simultaneous stimulation of osteoblast-mediated bone formation and osteoclast-mediated bone resorption in recipient OVX mice.

Stem cell homing capacity to the site of tissue injury is important for effective stem cell therapy. When hASCs labelled with Qtracker-delivered quantum dots were injected into OVX mice on post-operative day 28, a quantum dot signal could not be detected in bone at 60 min. after injection (Fig. S4A). A control experiment was performed with an experimental ischemia model in rat kidney to evaluate our system for assessment of the distribution of hASCs. Intense fluorescence from Qtracker labels and iron-labelled cells could be clearly seen at the ischemic site after injection of quantum-dot labelled or iron-labelled hASCs into ischemic kidney rats *via* tail vein (Fig. S4B and C). These results demonstrate that hASCs can move promptly into the damaged site in an acute ischemia-induced kidney model, but were not able to move into bone of OVX-induced osteoporotic mice. We made a profound attempt to identify localization of transplanted hASCs in a whole tissue. Among various tissues, tissue sections made from tibias of OVX mice following intravenous administration of hASCs showed that the transplanted cells were localized in the periosteum, but not in cortical bone. Periosteum is located at the outer bone surface along the periosteal cortex of cortical bone, and periosteal bone apposition plays a critical role in skeletal development [33]. Periosteum has been reported to show a dramatic response to bone growth factors with a significant increase in new bone formation. However, the question of whether or not the position of hASCs on periosteum specifically targeted a nearby part of the damaged bone is obscure. Our findings suggest that hASCs might not be directly involved in transdifferentiation into osteoblasts in trabecular and cortical bones. Instead, secreted factors from hASCs that are located sporadically all over the body and/or located in periosteum of the damaged bone tissue might be implicated in bone regeneration.

Synthesis of $VitD_3$ has been reported to occur in bone cells [34], and stimulation of osteoblast matrix mineralization by HGF in concert with $VitD_3$ has also been reported [35]. Our study showed that hASC-CM together with $VitD_3$-induced mineralization of

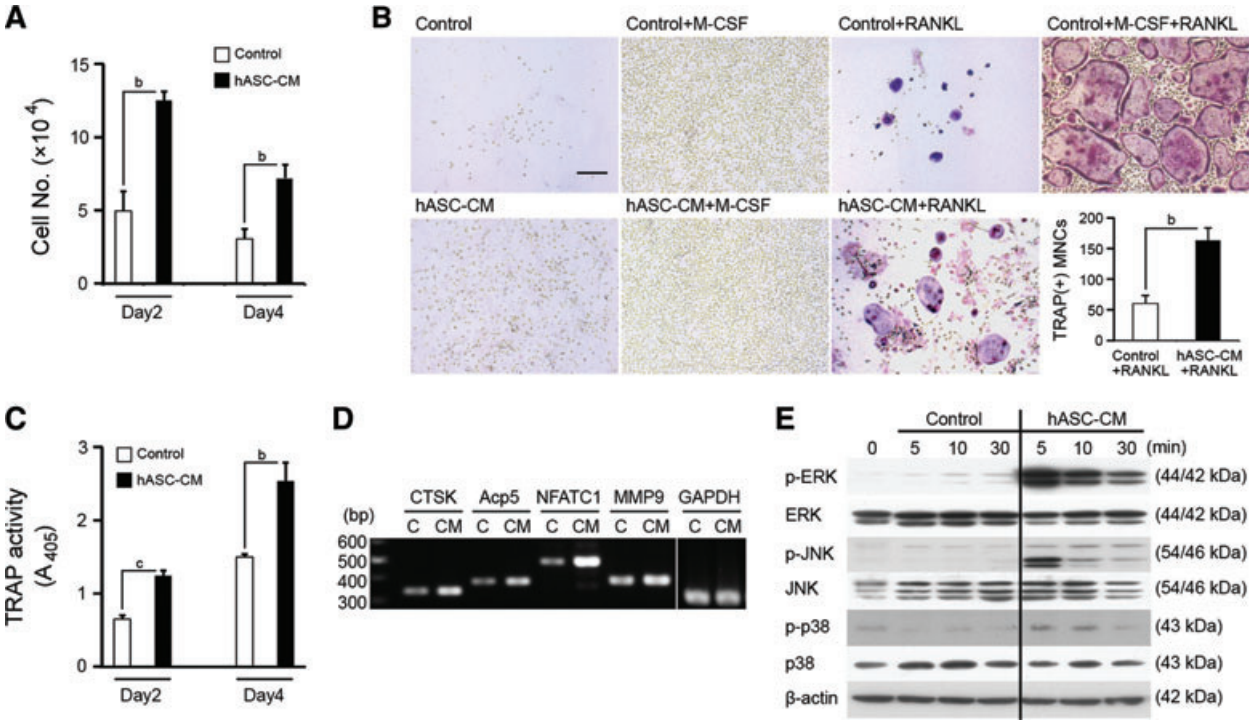

Fig. 5 Stimulatory action of hASC-CM in survival and differentiation of osteoclast precursor cells. (**A**) Osteoclast precursor survival. Osteoclast precursors (2×10^5 cells per well in 6-well plates) were cultured in the presence of 50% hASC-CM for the indicated times and trypan blue-excluded viable cells were then counted using a haemocytometer. Data represent mean ± S.D. ($n = 3$). (**B**) Osteoclast differentiation. Osteoclast precursors (5×10^4 cells per well in 48-well plates) were cultured for 8 days in control medium or in 50% hASC-CM in the presence or absence of M-CSF (30 ng/ml) or RANKL (50 ng/ml), as indicated. Media were replenished on day 2. After 8 days, cells were stained with TRAP and the number of $TRAP^+$ MNCs (>3 nuclei) was counted. Data represent mean ± S.D. ($n = 3$). Representative images of three independent experiments are presented. Scale bar: 100 μm. (**C**) TRAP activity. Osteoclast precursors (2×10^5 cells per well in 6-well plates) were incubated for the indicated times in control medium or in 50% hASC-CM and subjected to the TRAP assay. Data are representative of three independent experiments and expressed as mean ± S.D. ($n = 3$). (**D**) Osteoclast-specific gene expression. Osteoclast precursors were cultured in 50% hASC-CM for 2 days and the mRNA level for osteoclast marker genes was then determined using RT-PCR. Data are representative of three independent experiments. (**E**) Osteoclast-stimulating signals. Following adaption of osteoclast precursors for 12 hrs in the presence of M-CSF (30 ng/ml) and further incubation without M-CSF for 6 hrs, cells were stimulated with control medium or 50% hASC-CM for the indicated times and immediate responding signals in osteoclast precursors were analysed by Western blotting with specific antibodies to p-ERK, p-JNK and p-p38. β-actin was used as a loading control. The gel is representative of three independent experiments. b: $P < 0.01$; c: $P < 0.001$.

osteoblast cells, indicating the possibility that the combination of HGF secreted from hASCs and $VitD_3$ produced by bone cells plays an important role in osteoblast differentiation *in vivo*. Cellular adhesion to extracellular matrix is known to be essential to osteoblast survival, proliferation and differentiation [20]. In our experiments, cell attachment and spreading in osteoblasts were markedly increased by treatment with hASC-CM, and those increased activities were attenuated in the presence of EDTA, demonstrating that hASC-CM promotes adhesion and spreading of osteoblasts in a divalent cation-dependent manner. Integrins expressed on the plasma membrane of osteoblasts are known to require extracellular divalent cations in order to bind to their ligands [36], and interaction of integrin with extracellular matrix components activates osteoblast survival and matrix mineralization [20]. Therefore, various extracellular matrix proteins in hASC-CM, including fibronectin and type I collagen are likely to participate not only in cell adhesion, but also in proliferation and differentiation of osteoblast cells *via* integrin signalling.

Because M-CSF and RANKL are known to be critical for survival and differentiation of osteoclasts, and were detected in hASC-CM, we expected that survival and differentiation of osteoclast precursors might be induced by hASC-CM. Indeed, we found that hASC-CM was able to maintain the survival of osteoclast precursors. However, hASC-CM failed to direct the differentiation of osteoclast precursors into $TRAP^+$ MNCs. Compared with precursors cultured in control medium and RANKL, osteoclast precursors cultured in hASC-CM and RANKL formed much higher numbers of $TRAP^+$ MNCs. In the presence of RANKL, HGF has been shown to support osteoclast differentiation in a manner similar to that of M-CSF [37]. In addition, HGF receptor was expressed by both

osteoblasts and osteoclasts [17]. Therefore, our findings suggest that HGF, or M-CSF, or both in hASC-CM might be able to support proliferation and differentiation of osteoclast precursors, but that the level of RANKL in hASC-CM was not sufficient to induce osteoclastogenesis *in vitro*. These results are consistent with those of a previous report showing that ASCs could support differentiation of haematopoietic progenitor cells [8]. Involvement of ERK in osteoclast survival has been reported [38], and involvement of p38 and JNI in osteoclast differentiation has also been reported [39, 40]. ERK, JNK and p38 were strongly activated in response to hASC-CM in osteoclast precursors, implying that paracrine factors released by hASC could transiently activate all three major MAPKs (ERK, JNK and p38) that contribute to induction of osteoclastogenesis. In addition, hASC-CM induced maximal activation of ERK and JNK at day 3 after osteoblast culture. Taken together, these results suggest that enhanced survival and differentiation of osteoblasts and osteoclasts in cultures containing hASC-CM were mediated, at least in part, by activation of MAPKs.

Key mechanisms by which ASCs might repair and regenerate damaged tissues have been suggested to include paracrine effects of secreted cytokines and growth factors, and direct differentiation to a desired cell lineage [5]. In a developing mouse model, differentiation into osteoblasts appears to be especially important for treatment of osteogenesis imperfecta [41]. However, hASC-induced improvement of bone mass could not be fully explained by direct differentiation into osteoblasts because hASC-injected OVX mice exhibit increased numbers of both osteoblasts and mature osteoclasts, and hASC-CM simultaneously stimulates proliferation and differentiation of both osteoblasts and osteoclasts *in vitro*. Based on *in vivo* and *in vitro* results from our adult mouse model, we suggest that paracrine effects induced by systemic transplantation of hASCs are the predominant mechanism mediating the therapeutic effects of hASCs in treatment of osteoporosis. Collectively, hASCs transplanted *via* the circulatory system could function as antiresorptive and anabolic agents, and could be a valuable therapeutic option for treatment of both high- and low-turnover osteoporosis.

Acknowledgements

This work was supported, in part, by grants from the Korea Healthcare Technology R&D Project, Ministry for Health, Welfare & Family Affairs, Republic of Korea (A084221; to D.J.) and from the Korea Science and Engineering Foundation (No. 2010–0001240).

Conflict of interest

The authors confirm that there are no conflicts of interest.

Supporting Information

Additional Supporting Information may be found in the online version of this article:

Fig. S1 Flow cytometric analysis for cell surface marker expression in hASCs.

Fig. S2 Multilineage differentiation capacity of hASCs.

Fig. S3 Measurement of uterus thickness in sham-operated (Sham) and OVX mice systemically transplanted with or without hASCs.

Fig. S4 Localization of hASCs after systemic transplantation.

Table S1 Primers used in this study

Table S2 Mass spectrometric identification of proteins secreted by hASCs using a gel-based approach

Table S3 Mass spectrometric identification of proteins secreted by hASCs using a non-gel based approach

Please note: Wiley-Blackwell is not responsible for the content or functionality of any supporting materials supplied by the authors. Any queries (other than missing material) should be directed to the corresponding author for the article.

References

1. **Raisz LG.** Pathogenesis of osteoporosis: concepts, conflicts, and prospects. *J Clin Invest*. 2005; 115: 3318–25.
2. **Zaidi M.** Skeletal remodeling in health and disease. *Nat Med*. 2007; 13: 791–801.
3. **Mimeault M, Batra SK.** Concise review: recent advances on the significance of stem cells in tissue regeneration and cancer therapies. *Stem Cells*. 2006; 24: 2319–45.
4. **Mimeault M, Batra SK.** Recent progress on tissue-resident adult stem cell biology and their therapeutic implications. *Stem Cell Rev*. 2008; 4: 27–49.
5. **Gimble JM, Katz AJ, Bunnell BA.** Adipose-derived stem cells for regenerative medicine. *Circ Res*. 2007; 100: 1249–60.
6. **Lien CY, Chih-Yuan Ho K, Lee OK, *et al.*** Restoration of bone mass and strength in glucocorticoid-treated mice by systemic transplantation of CXCR4 and cbfa-1 co-expressing mesenchymal stem cells. *J Bone Miner Res*. 2009; 24: 837–48.
7. **Zuk PA, Zhu M, Ashjian P, *et al.*** Human adipose tissue is a source of multipotent stem cells. *Mol Biol Cell*. 2002; 13: 4279–95.
8. **Corre J, Barreau C, Cousin B, *et al.*** Human subcutaneous adipose cells support complete differentiation but not self-renewal of hematopoietic progenitors. *J Cell Physiol*. 2006; 208: 282–8.
9. **Cai L, Johnstone BH, Cook TG, *et al.*** IFATS collection: human adipose tissue-derived stem cells induce angiogenesis

and nerve sprouting following myocardial infarction, in conjunction with potent preservation of cardiac function. *Stem Cells*. 2009; 27: 230–7.

10. **Rehman J, Traktuev D, Li J, *et al.*** Secretion of angiogenic and antiapoptotic factors by human adipose stromal cells. *Circulation*. 2004; 109: 1292–8.
11. **Kilroy GE, Foster SJ, Wu X, *et al.*** Cytokine profile of human adipose-derived stem cells: expression of angiogenic, hematopoietic, and pro-inflammatory factors. *J Cell Physiol*. 2007; 212: 702–9.
12. **Wei X, Zhao L, Zhong J, *et al.*** Adipose stromal cells-secreted neuroprotective media against neuronal apoptosis. *Neurosci Lett*. 2009; 462: 76–9.
13. **Lee K, Kye M, Jang JS, *et al.*** Proteomic analysis revealed a strong association of a high level of alpha1-antitrypsin in gastric juice with gastric cancer. *Proteomics*. 2004; 4: 3343–52.
14. **Kim H, Choi HK, Shin JH, *et al.*** Selective inhibition of RANK blocks osteoclast maturation and function and prevents bone loss in mice. *J Clin Invest*. 2009; 119: 813–25.
15. **Lee SH, Rho J, Jeong D, *et al.*** v-ATPase V0 subunit d2-deficient mice exhibit impaired osteoclast fusion and increased bone formation. *Nat Med*. 2006; 12: 1403–9.
16. **Huh YJ, Kim JM, Kim H, *et al.*** Regulation of osteoclast differentiation by the redox-dependent modulation of nuclear import of transcription factors. *Cell Death Differ*. 2006; 13: 1138–46.
17. **Grano M, Galimi F, Zambonin G, *et al.*** Hepatocyte growth factor is a coupling factor for osteoclasts and osteoblasts *in vitro*. *Proc Natl Acad Sci USA*. 1996; 93: 7644–8.
18. **Delany AM, Kalajzic I, Bradshaw AD, *et al.*** Osteonectin-null mutation compromises osteoblast formation, maturation, and survival. *Endocrinology*. 2003; 144: 2588–96.
19. **Zhu S, Barbe MF, Liu C, *et al.*** Periostin-like-factor in osteogenesis. *J Cell Physiol*. 2009; 218: 584–92.
20. **Globus RK, Doty SB, Lull JC, *et al.*** Fibronectin is a survival factor for differentiated osteoblasts. *J Cell Sci*. 1998; 111: 1385–93.
21. **Menaa C, Esser E, Sprague SM.** Beta2-microglobulin stimulates osteoclast formation. *Kidney Int*. 2008; 73: 1275–81.
22. **Carron JA, Wagstaff SC, Gallagher JA, *et al.*** A CD36-binding peptide from thrombospondin-1 can stimulate resorption by osteoclasts *in vitro*. *Biochem Biophys Res Commun*. 2000; 270: 1124–7.
23. **Datta NS, Abou-Samra AB.** PTH and PTHrP signaling in osteoblasts. *Cell Signal*. 2009; 21: 1245–54.
24. **Weitzmann MN, Pacifici R.** Estrogen deficiency and bone loss: an inflammatory tale. *J Clin Invest*. 2006; 116: 1186–94.
25. **Scutt A, Bertram P.** Bone marrow cells are targets for the anabolic actions of prostaglandin E2 on bone: induction of a transition from nonadherent to adherent osteoblast precursors. *J Bone Miner Res*. 1995; 10: 474–87.
26. **Rickard DJ, Kazhdan I, Leboy PS.** Importance of 1,25-dihydroxyvitamin D3 and the nonadherent cells of marrow for osteoblast differentiation from rat marrow stromal cells. *Bone*. 1995; 16: 671–8.
27. **Ogasawara T, Kawaguchi H, Jinno S, *et al.*** Bone morphogenetic protein 2-induced osteoblast differentiation requires Smad-mediated down-regulation of Cdk6. *Mol Cell Biol*. 2004; 24: 6560–8.
28. **Chang J, Wang Z, Tang E, *et al.*** Inhibition of osteoblastic bone formation by nuclear factor-kappaB. *Nat Med*. 2009; 15: 682–9.
29. **Kim WS, Park BS, Sung JH, *et al.*** Wound healing effect of adipose-derived stem cells: a critical role of secretory factors on human dermal fibroblasts. *J Dermatol Sci*. 2007; 48: 15–24.
30. **Nakagami H, Maeda K, Morishita R, *et al.*** Novel autologous cell therapy in ischemic limb disease through growth factor secretion by cultured adipose tissue-derived stromal cells. *Arterioscler Thromb Vasc Biol*. 2005; 25: 2542–7.
31. **Einhorn TA.** The cell and molecular biology of fracture healing. *Clin Orthop Relat Res*. 1998: S7–21.
32. **Lieberman JR, Daluiski A, Einhorn TA.** The role of growth factors in the repair of bone. Biology and clinical applications. *J Bone Joint Surg Am*. 2002; 84-A: 1032–44.
33. **Allen MR, Hock JM, Burr DB.** Periosteum: biology, regulation, and response to osteoporosis therapies. *Bone*. 2004; 35: 1003–12.
34. **Howard GA, Turner RT, Sherrard DJ, *et al.*** Human bone cells in culture metabolize 25-hydroxyvitamin D3 to 1,25-dihydroxyvitamin D3 and 24,25-dihydroxyvitamin D3. *J Biol Chem*. 1981; 256: 7738–40.
35. **D'Ippolito G, Schiller PC, Perez-stable C, *et al.*** Cooperative actions of hepatocyte growth factor and 1,25-dihydroxyvitamin D3 in osteoblastic differentiation of human vertebral bone marrow stromal cells. *Bone*. 2002; 31: 269–75.
36. **Smith JW, Piotrowicz RS, Mathis D.** A mechanism for divalent cation regulation of beta 3-integrins. *J Biol Chem*. 1994; 269: 960–7.
37. **Adamopoulos IE, Xia Z, Lau YS, *et al.*** Hepatocyte growth factor can substitute for M-CSF to support osteoclastogenesis. *Biochem Biophys Res Commun*. 2006; 350: 478–83.
38. **Miyazaki T, Katagiri H, Kanegae Y, *et al.*** Reciprocal role of ERK and NF-kappaB pathways in survival and activation of osteoclasts. *J Cell Biol*. 2000; 148: 333–42.
39. **Matsumoto M, Sudo T, Saito T, *et al.*** Involvement of p38 mitogen-activated protein kinase signaling pathway in osteoclastogenesis mediated by receptor activator of NF-kappa B ligand (RANKL). *J Biol Chem*. 2000; 275: 31155–61.
40. **David JP, Sabapathy K, Hoffmann O, *et al.*** JNK1 modulates osteoclastogenesis through both c-Jun phosphorylation-dependent and -independent mechanisms. *J Cell Sci*. 2002; 115: 4317–25.
41. **Li F, Wang X, Niyibizi C.** Distribution of single-cell expanded marrow derived progenitors in a developing mouse model of osteogenesis imperfecta following systemic transplantation. *Stem Cells*. 2007; 25: 3183–93.
42. **Lynch MP, Stein JL, Stein GS, *et al.*** The influence of type I collagen on the development and maintenance of the osteoblast phenotype in primary and passaged rat calvarial osteoblasts: modification of expression of genes supporting cell growth, adhesion, and extracellular matrix mineralization. *Exp Cell Res*. 1995; 216: 35–45.
43. **Hankenson KD, Bornstein P.** The secreted protein thrombospondin 2 is an autocrine inhibitor of marrow stromal cell proliferation. *J Bone Miner Res*. 2002; 17: 415–25.
44. **Thapa N, Kang KB, Kim IS.** Beta ig-h3 mediates osteoblast adhesion and inhibits differentiation. *Bone*. 2005; 36: 232–42.
45. **Xu K, Zhang Y, Ilalov K, *et al.*** Cartilage oligomeric matrix protein associates with granulin-epithelin precursor (GEP) and potentiates GEP-stimulated chondrocyte proliferation. *J Biol Chem*. 2007; 282: 11347–55.
46. **Hayami T, Kapila YL, Kapila S.** MMP-1 (collagenase-1) and MMP-13 (collagenase-3) differentially regulate markers of osteoblastic differentiation in osteogenic cells. *Matrix Biol*. 2008; 27: 682–92.

47. **Mosig RA, Dowling O, DiFeo A, *et al.*** Loss of MMP-2 disrupts skeletal and craniofacial development and results in decreased bone mineralization, joint erosion and defects in osteoblast and osteoclast growth. *Hum Mol Genet*. 2007; 16: 1113–23.
48. **Nordstrom SM, Carleton SM, Carson WL, *et al.*** Transgenic over-expression of plasminogen activator inhibitor-1 results in age-dependent and gender-specific increases in bone strength and mineralization. *Bone*. 2007; 41: 995–1004.
49. **Everts V, Korper W, Hoeben KA, *et al.*** Osteoclastic bone degradation and the role of different cysteine proteinases and matrix metalloproteinases: differences between calvaria and long bone. *J Bone Miner Res*. 2006; 21: 1399–408.
50. **Matsumoto N, Jo OD, Shih RN, *et al.*** Increased cathepsin D release by Hyp mouse osteoblast cells. *Am J Physiol Endocrinol Metab*. 2005; 289: E123–32.
51. **Raouf A, Ganss B, McMahon C, *et al.*** Lumican is a major proteoglycan component of the bone matrix. *Matrix Biol*. 2002; 21: 361–7.
52. **Zambuzzi WF, Yano CL, Cavagis AD, *et al.*** Ascorbate-induced osteoblast differentiation recruits distinct MMP-inhibitors: RECK and TIMP-2. *Mol Cell Biochem*. 2009; 322: 143–50.
53. **Geoffroy V, Marty-Morieux C, Le Goupil N, *et al.*** *In vivo* inhibition of osteoblastic metalloproteinases leads to increased trabecular bone mass. *J Bone Miner Res*. 2004; 19: 811–22.